Carbons

Carbon – Phase Diagram

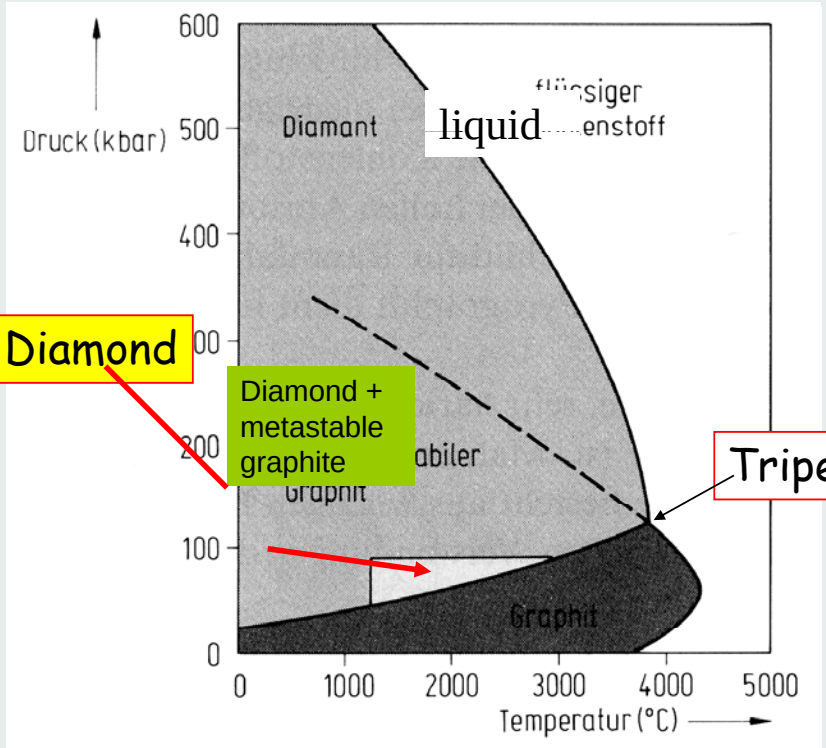

Graphite → Diamond

Diamond + metastable graphite

Tripelpoint

R. NESPER ETH ZÜRICH & COLLEGIUM HELVETICUM

31.10.2007

Tetrels – Phase Diagrams

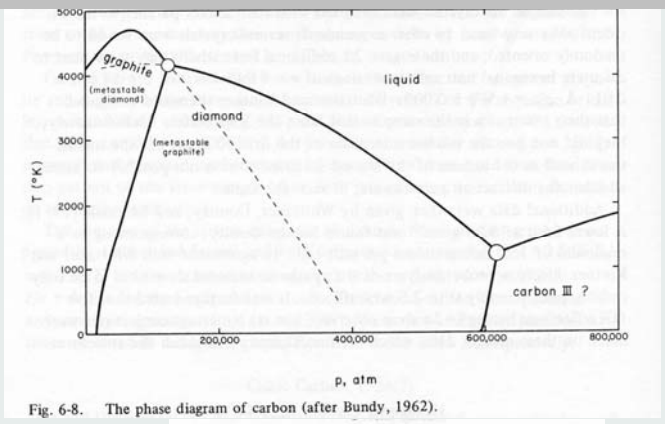

Fig. 6-8. The phase diagram of carbon (after Bundy, 1962).

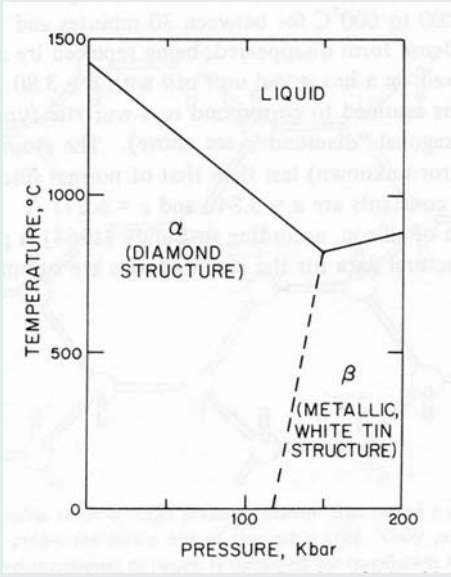

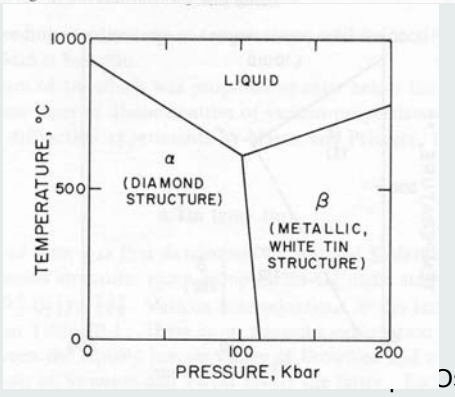

Cubic Diamond

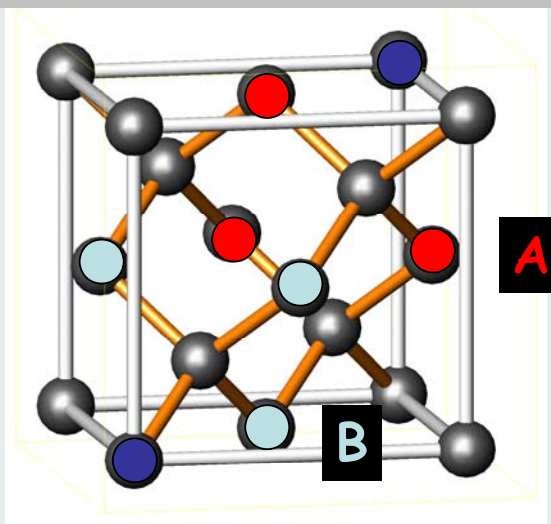

1.54Å
ΔH_B=348 kJmol^{-1}

at 1 bar, 25°C metastable; 1500°C: $C_{Diamant} \rightarrow C_{Graphit}$

Diamond

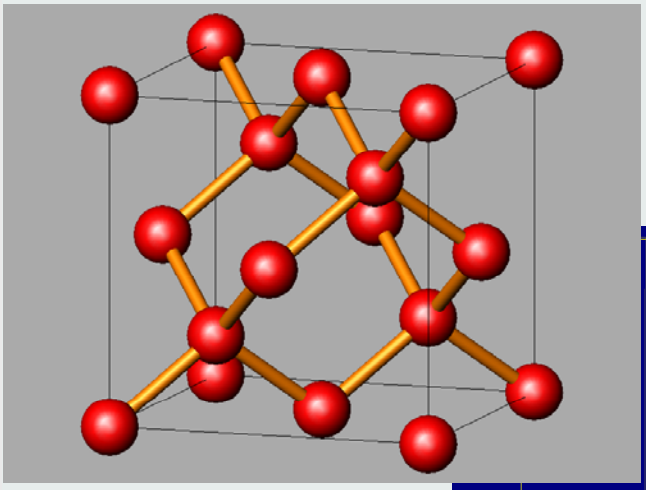

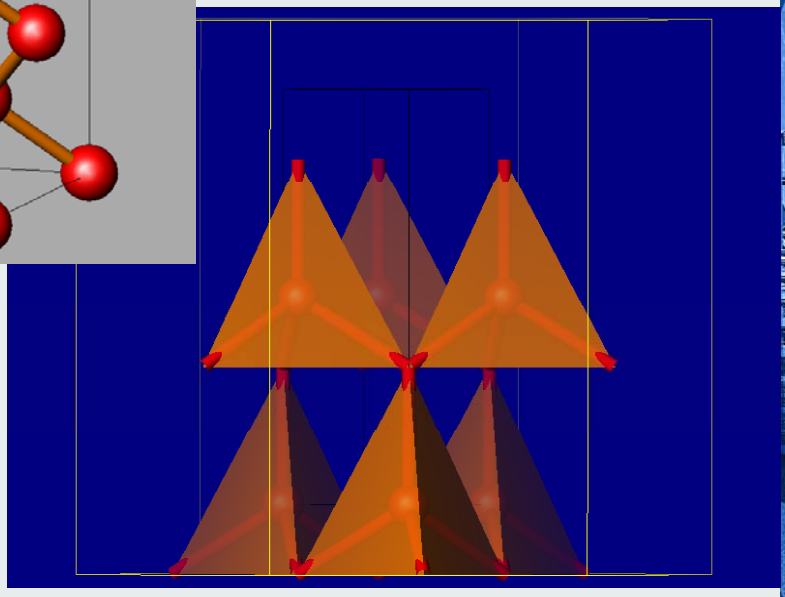

Hexagonal and Rhomboedral Graphite

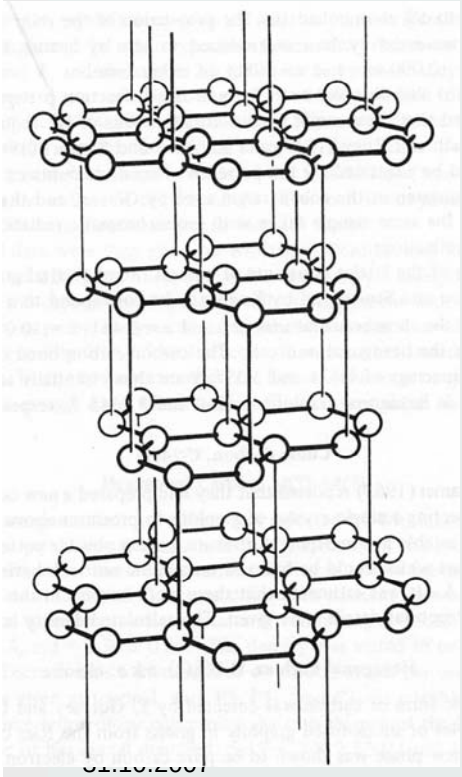

conductivity: $10^4\ \Omega^{-1}\ cm^{-1}$

$\approx 1\ \Omega^{-1}\ cm^{-1}$

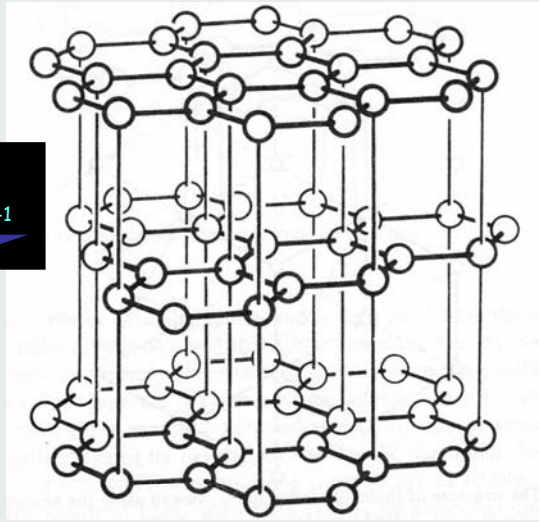

Electronic Conductivity of Graphite

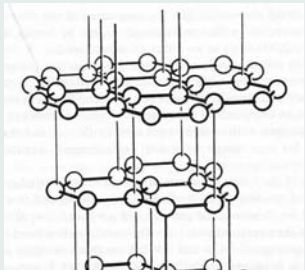

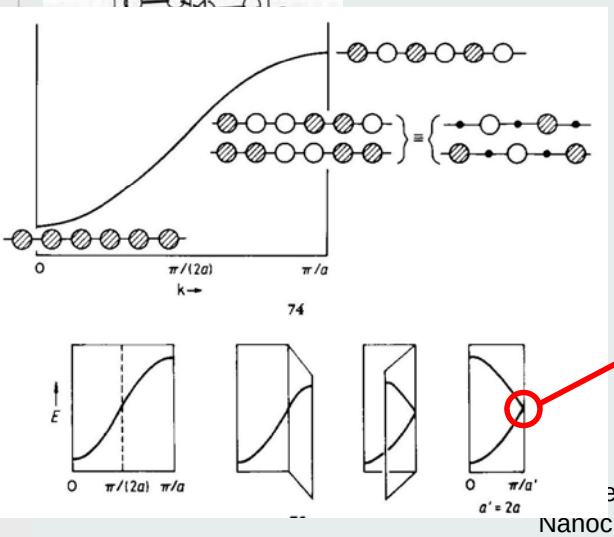

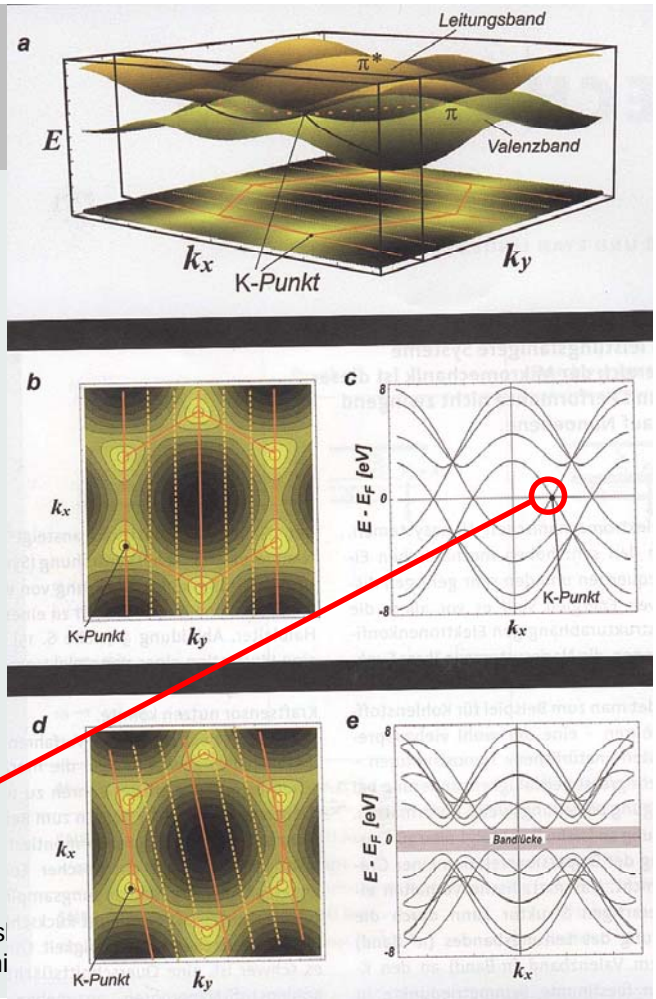

er Os
Nanochemi

Buckminster-Fullerenes

60 Corners

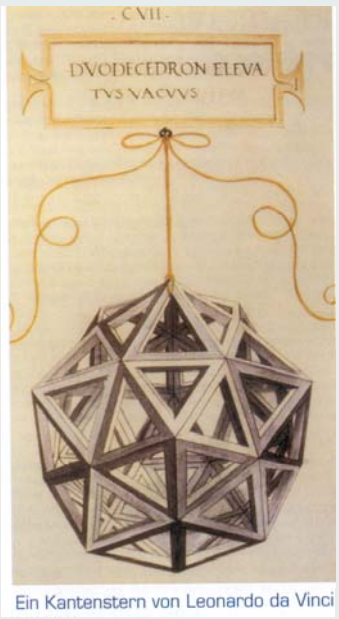

Ein Kantenstern von Leonardo da Vinci

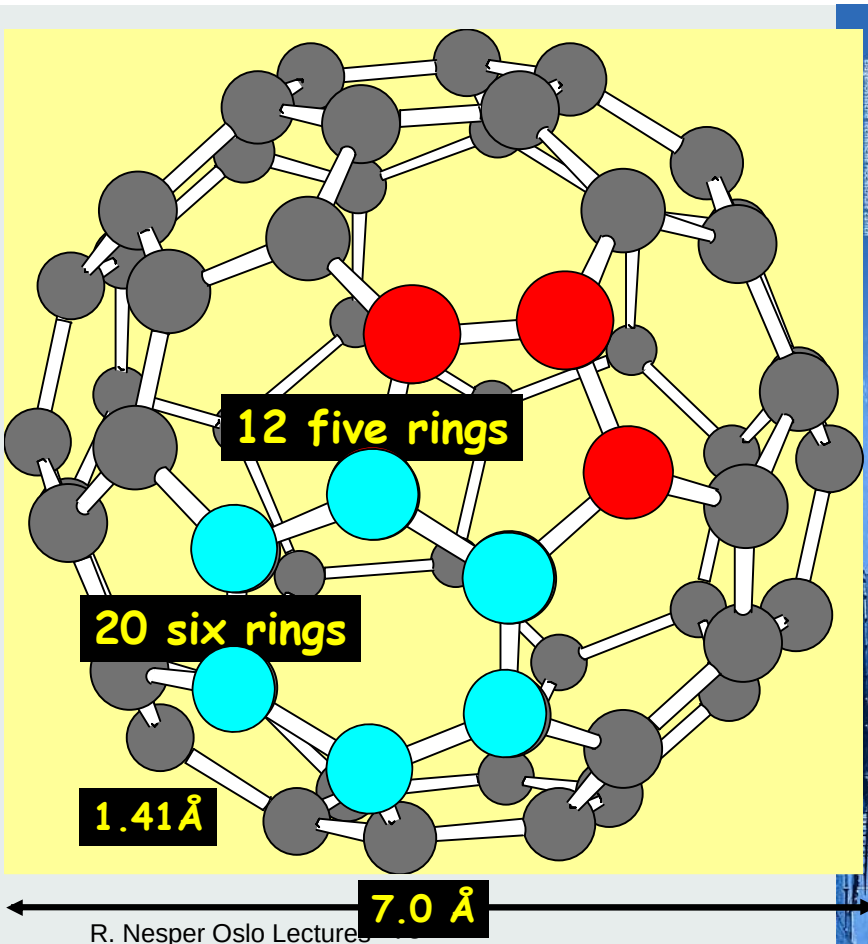

Fullerenes

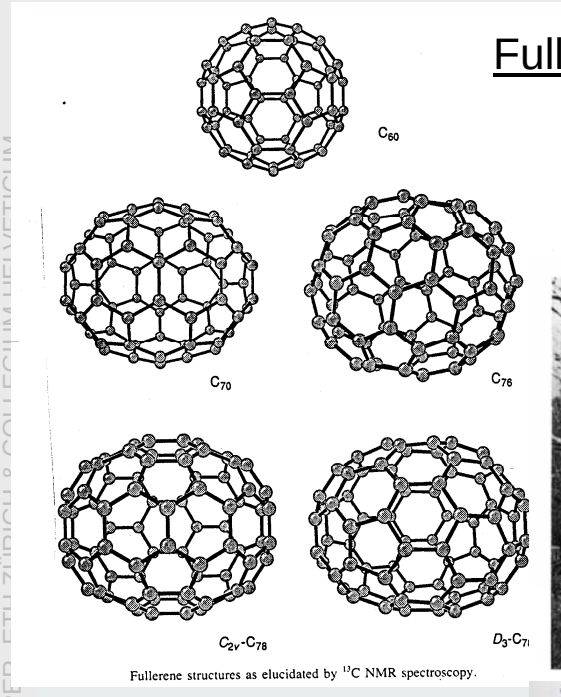

Fullerene structures as elucidated by ^{13}C NMR spectroscopy.

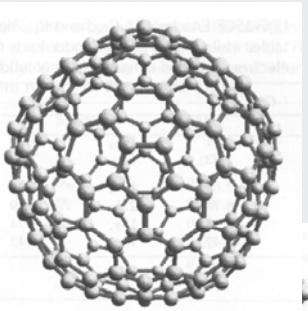

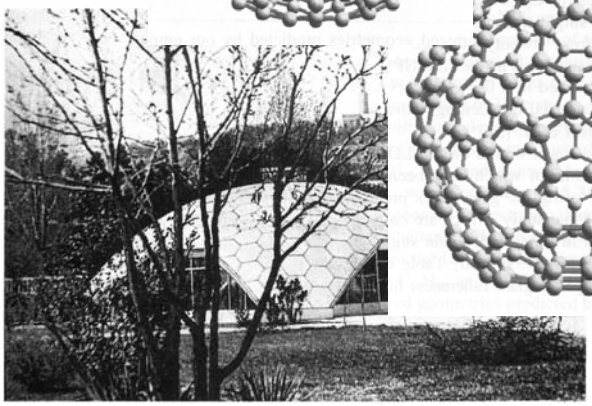

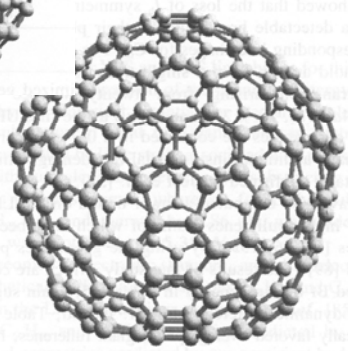

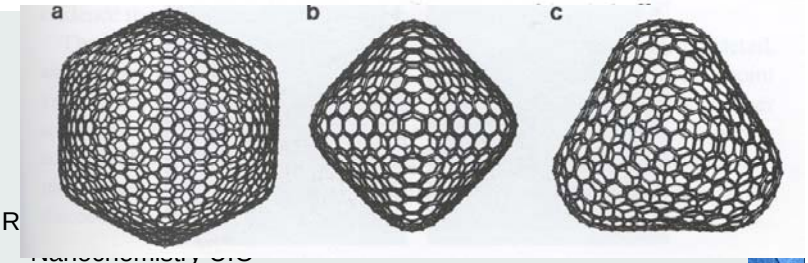

C-Fullerene to Diamond

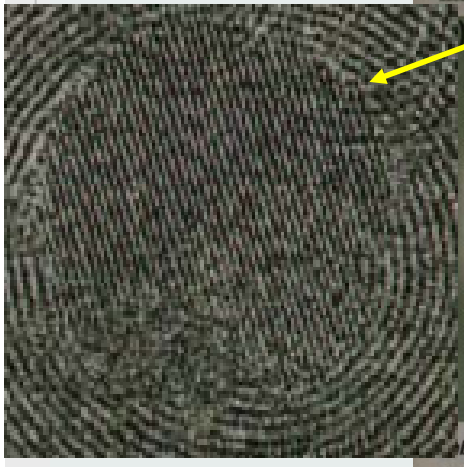

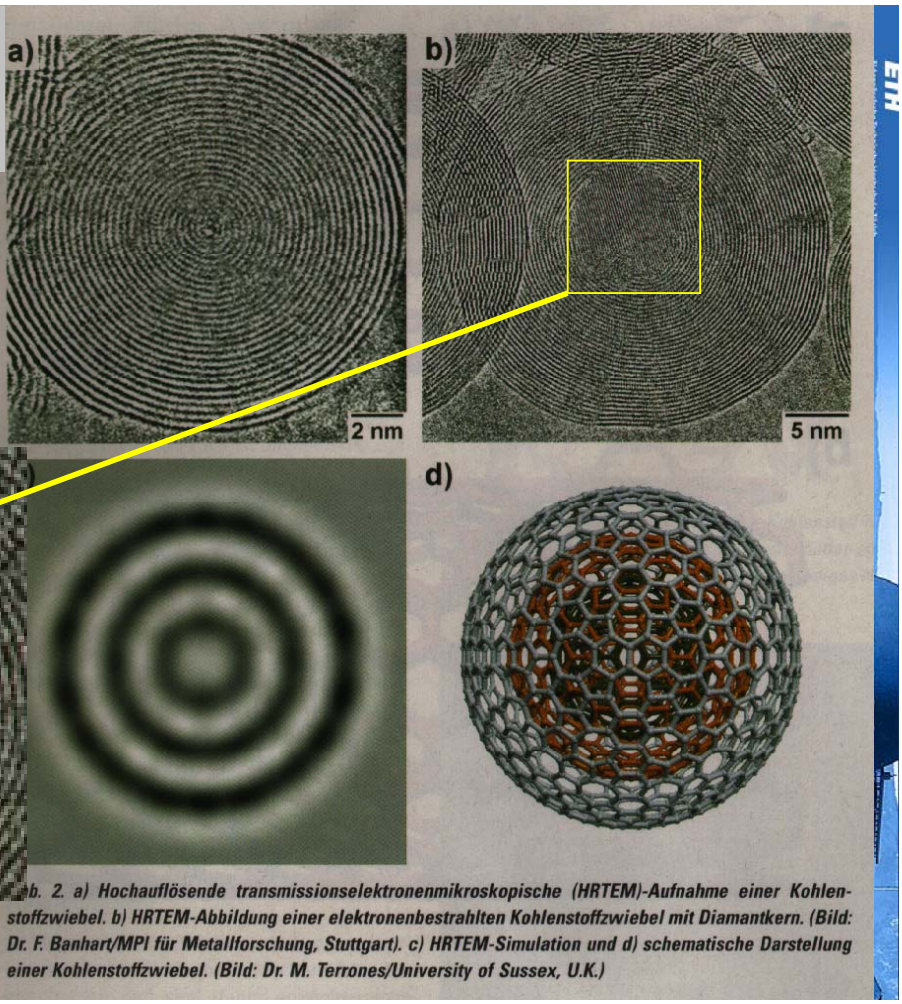

b. 2. a) Hochauflösende transmissionselektronenmikroskopische (HRTEM)-Aufnahme einer Kohlenstoffzwiebel. b) HRTEM-Abbildung einer elektronenbestrahlten Kohlenstoffzwiebel mit Diamantkern. (Bild: Dr. F. Banhart/MPI für Metallforschung, Stuttgart). c) HRTEM-Simulation und d) schematische Darstellung einer Kohlenstoffzwiebel. (Bild: Dr. M. Terrones/University of Sussex, U.K.)

Fullerenes

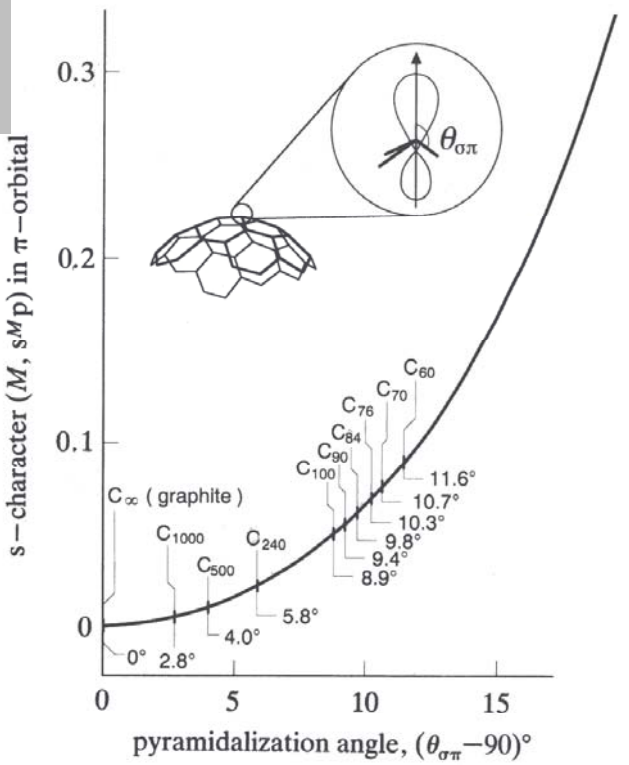

Figure 4. Rehybridization as a function of pyramidalization angle. The π-orbital axis vector (POAV1 approximation), is defined as that vector which makes equal angles to the three σ-bonds at a conjugated carbon atom (Haddon 1988). The common angle to the three σ-bonds (which are assumed to lie along the internuclear axes), is denoted $\theta_{\sigma\pi}$. The average pyramidalization angle $[(\overline{\theta_{\sigma\pi}} - 90)°]$ shown for representative fullerenes (C_n), was obtained from eqn (2) of Haddon *et al.* (1986*b*) for $n > 60$.

Fullerene Isomers

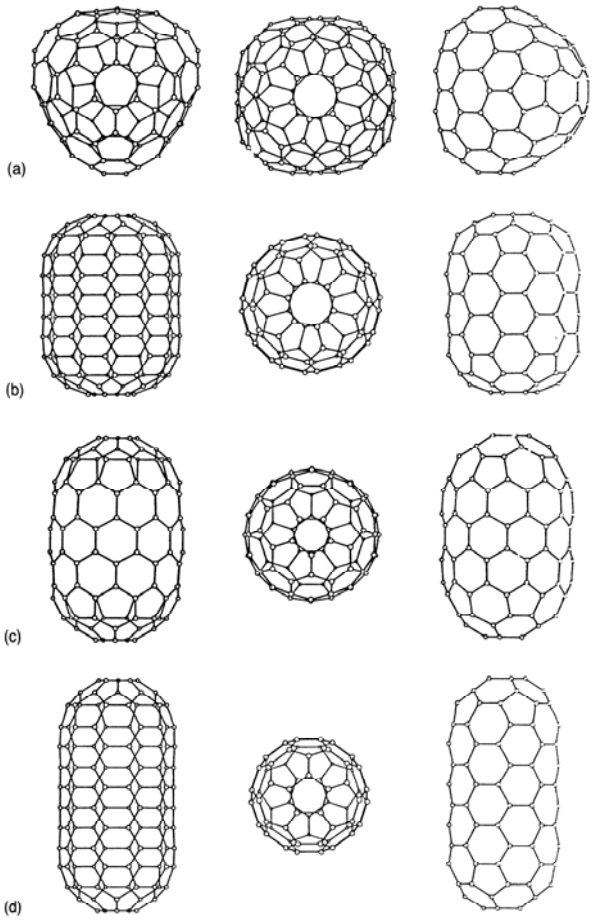

Figure 5.4 Equilibrium geometries of four isomers of C_{120} as predicted by the STO-3G/SCF level of theory: (a) T_d, (b) D_{6d}, (c) D_{5d} SF, (d) D_{5d} VF.

Fulleren – C_{60}

C_{60}: 12 Fünfringe + 20 Sechsringe

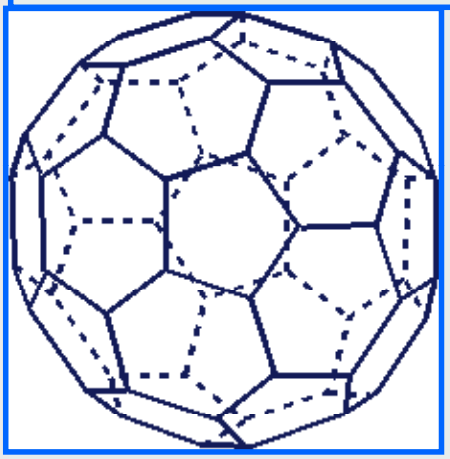

Es sollten 3N-6 = 3·60-6 = 174 Freiheitsgrade vorliegen

Aber nur 4 Schwingungsfrequenzen werden beobachtet!

Fulleren – C_{60} - Schwingungsspektren

IR= Infrarot; RE= Raman Effekt; RR= Resonanz-Raman-Effekt; HR= Hyper-Raman-Effekt

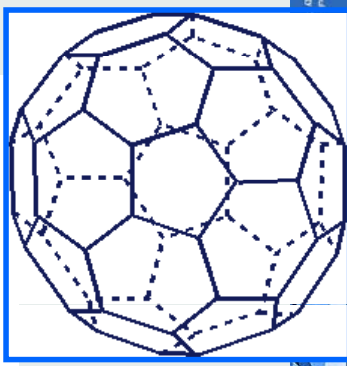

8.54 Punktgruppe I_h oder m 3 5 (2/m $\bar{3}$ $\bar{5}$)

Rasse	Aktivität IR	RE	RR	HR	Zahl der Grundschwingungen	Translation	Rotation
A_g	–	tp	tp	–	$r_5+r_3+r_2+2m_z+3n$		
A_u	–	–	–	–	m_z+3n		
F_{1g}	–	–	ip	–	$r_5+r_3+2r_2+4m_z+9n-1$		R_x, R_y, R_z
F_{1u}	a	–	–	p	$n_0+2r_5+2r_3+3r_2+5m_z+9n-1$	T_x, T_y, T_z	
F_{2g}	–	–	–	–	$r_3+2r_2+4m_z+9n$		
F_{2u}	–	–	–	dp	$r_5+2r_3+3r_2+5m_z+9n$		
G_g	–	–	–	–	$r_5+2r_3+3r_2+6m_z+12n$		
G_u	–	–	–	dp	$r_5+2r_3+3r_2+6m_z+12n$		
H_g	–	dp	dp	–	$2r_5+3r_3+4r_2+8m_z+15n$		
H_u	–	–	–	–	$r_5+2r_3+3r_2+7m_z+15n$		

$Z = n_0+12r_5+20r_3+30r_2+60m_z+120n$

Obertöne wie bei Punktgruppe *I* oder 235 unter zusätzlicher Berücksichtigung der *g-u*-Regel

Es sollten 3N-6 = 3·60-6 = 174 Freiheitsgrade vorliegen

Aber nur 4 Schwingungsfrequenzen werden beobachtet!

R. NESPER ETH ZÜRICH & COLLEGIUM HELVETICUM

Fullerene C_{60} Molecular Orbitals

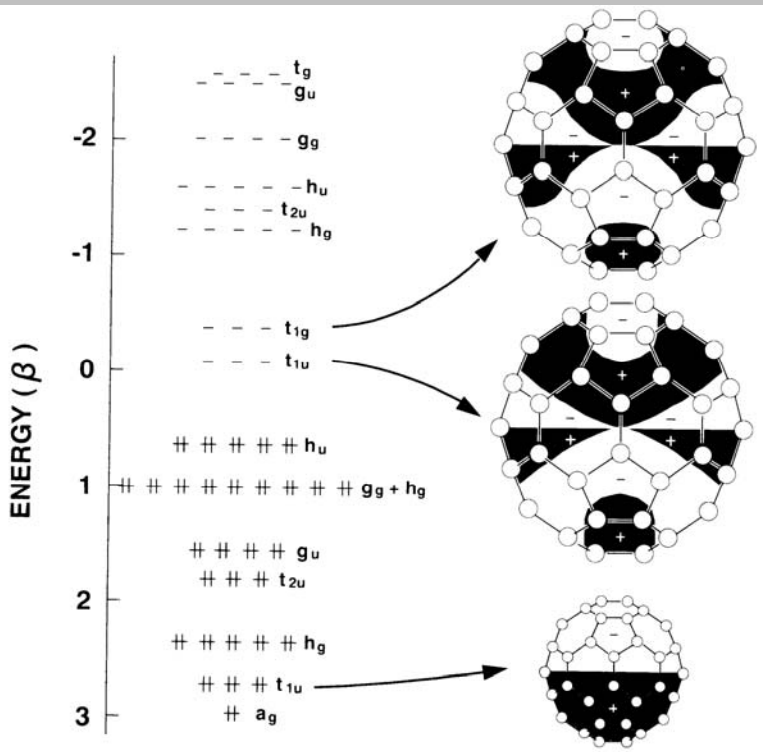

Fullerene Superconductors

M_3C_{60}

M=K, Rb

T_c (max) ~ 40K

1. Hückel molecular orbital (HMO) energy levels of C_{60} together with one component of the triply degenerate t_{1u} and t_{1g} sets of molecular orbitals.

Fullerene Compounds

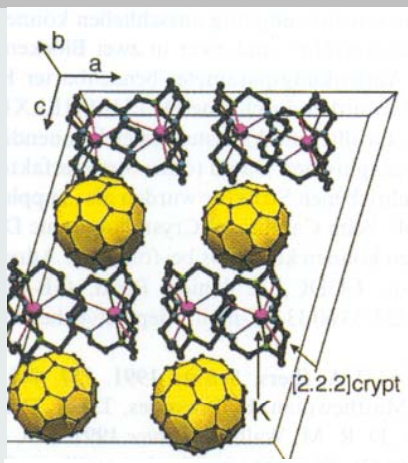

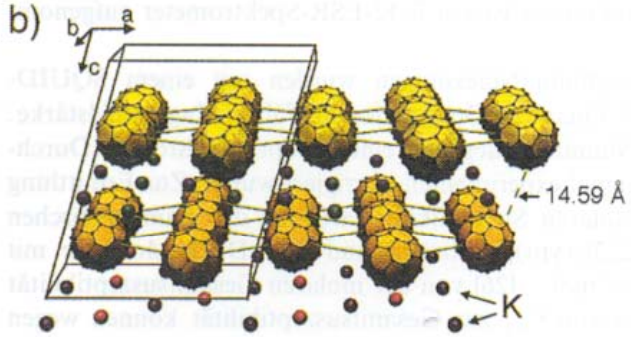

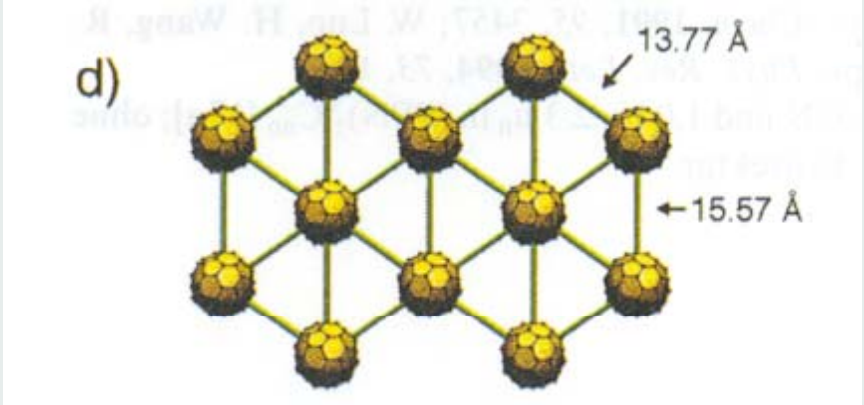

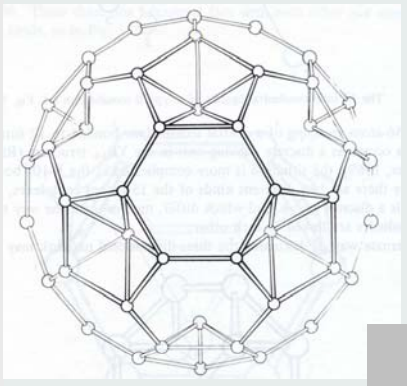

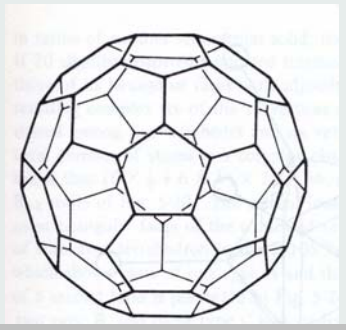

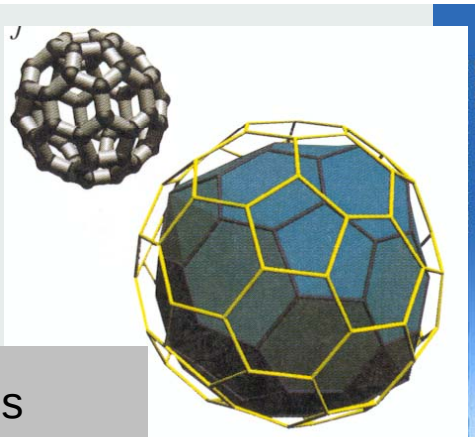

Metal Fulleranes

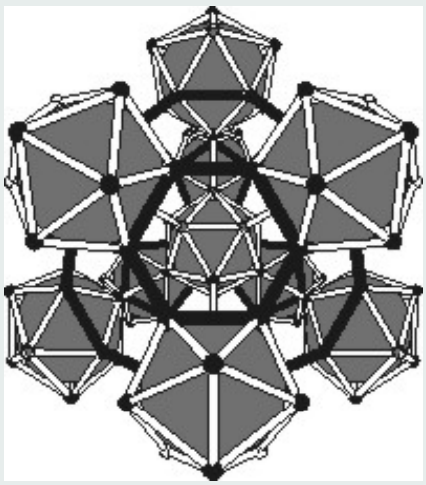

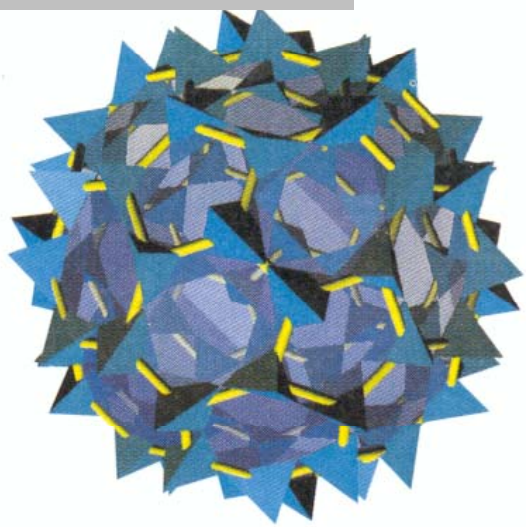

R. Nes
Nan

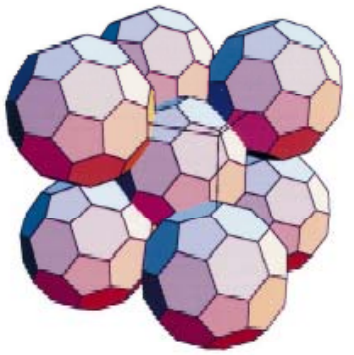

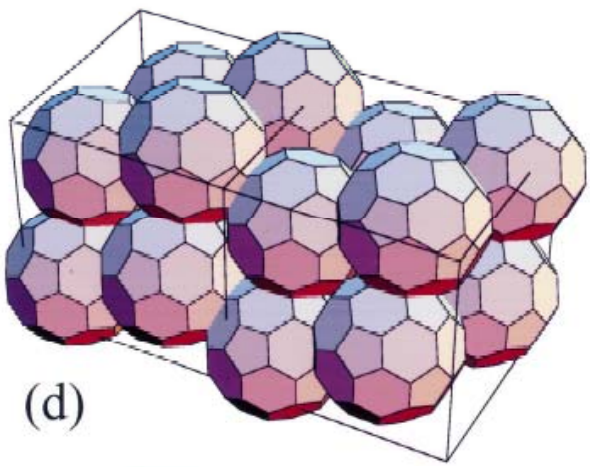

(a)

(d)

(b)

(c)

Fig. 2. The structures of two cubic Fibonacci approximants with Bergman clusters (BC) shown as solid soccer balls: (a) b.c.c. packing of BC in the crystal structure of 1/1-$(Al,Zn)_3Mg_2$; the connection of Bergman clusters as found in the 1/1- and 2/1-approximant: (b) clusters along twofold axes are connected via common edges (b bonds) and (c) along threefold axes via common hexagon faces (c bonds); (d) the rhombohedral packing of BCs at the vertices of prolate and oblate rhombohedra in the crystal structure of 2/1-$(Al,Zn)_{3+\delta}Mg_{2-\delta}$.

Stability of Fullerenes

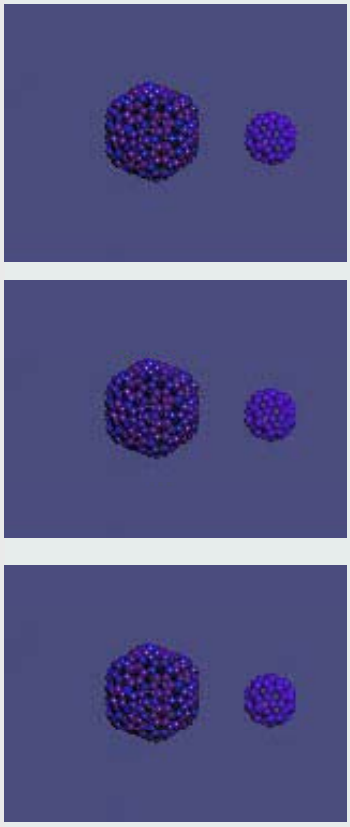

2 conformers of C_{240}

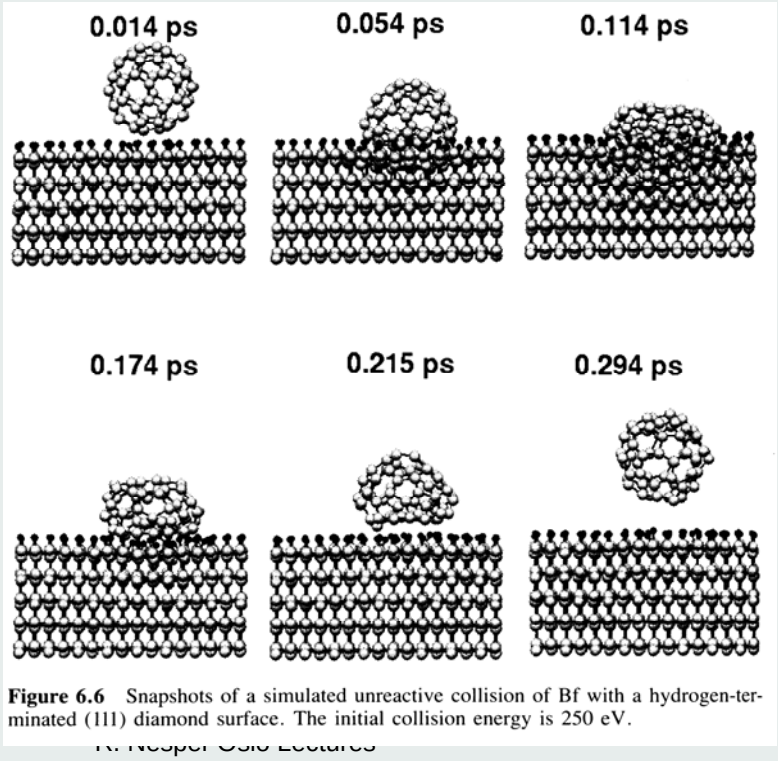

Figure 6.6 Snapshots of a simulated unreactive collision of Bf with a hydrogen-terminated (111) diamond surface. The initial collision energy is 250 eV.

More New Carbons to Come?

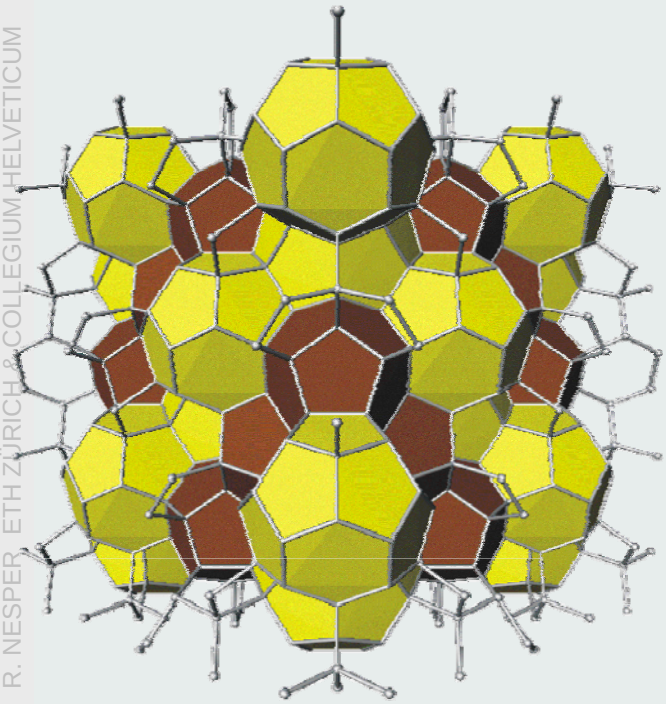

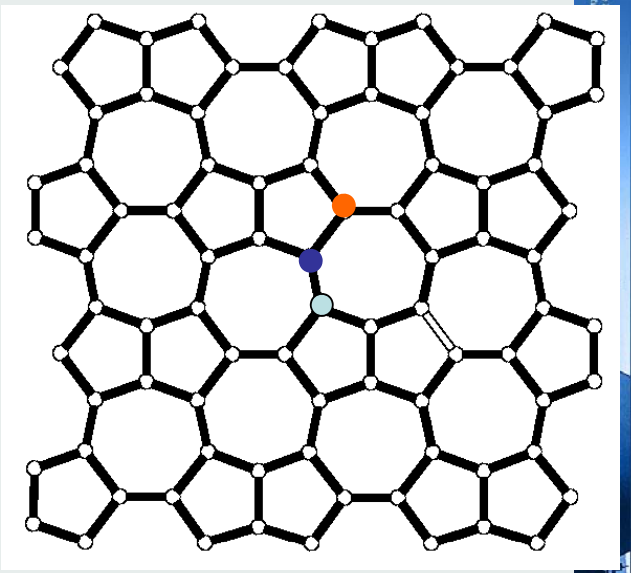

(7^25) (757) (75^2) net

Hyperbolic 3D Carbons – sp^3 Frameworks

Car-Parrinello-MD based on zeolite trial structures

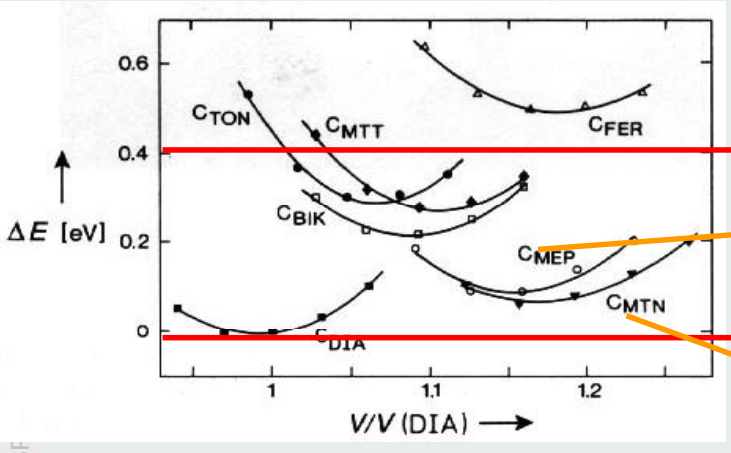

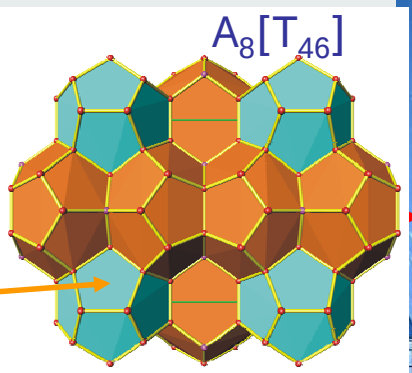

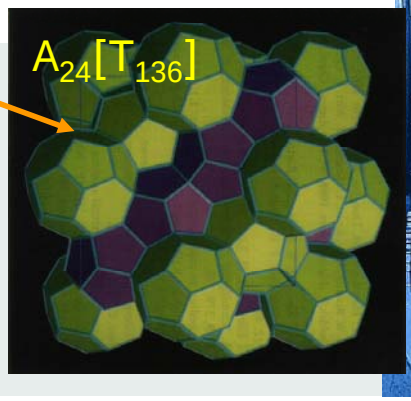

R. Nesper, K. Vogel, P. Blöchl, *Angew. Chem.* 1993, **105**, 786

Novel Hyperbolic Carbons – sp^2 Frameworks

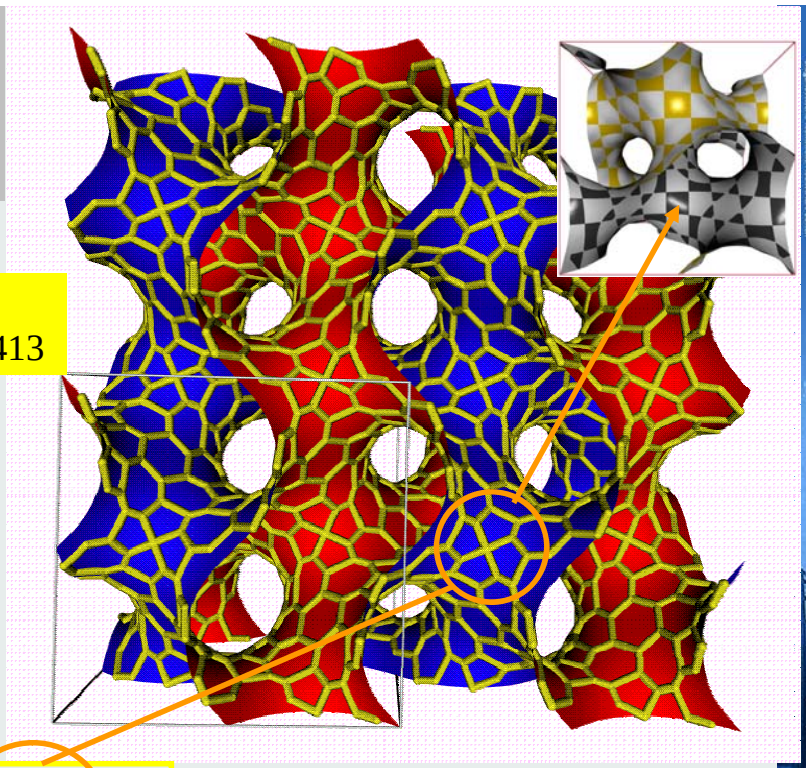

R. Nesper, S. Leoni
Chemphyschem **2001**, *2 (7)*, 413

$G[(76^2)(765)(755)(5^4)]$

Morel Novel sp^2 Carbons ?

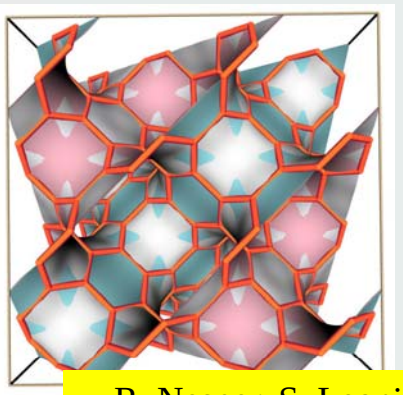

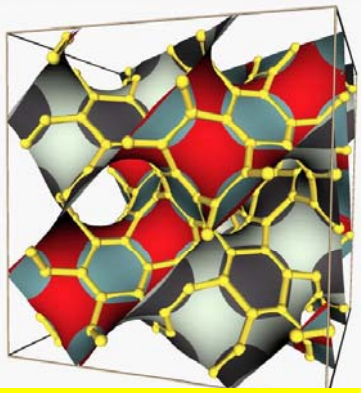

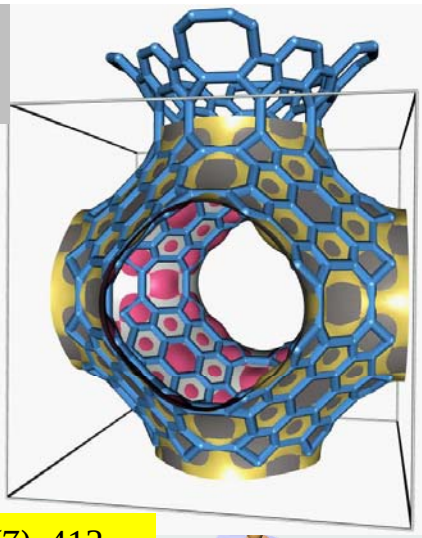

R. Nesper, S. Leoni, *Chemphyschem* **2001**, *2 (7)*, 413